RG&SA
Revista Gestão & Sustentabilidade Ambiental
Artigos

PRODUCTION AND CHARACTERIZATION OF ACTIVATED BIOCHAR OF *CÁSSIA FISTULA L.* LEAVES

DOI: http://dx.doi.org/10.19177/rgsa.v9e02020800-815

Fabíola Tomassoni[1]
Elisângela E. Schneider[2]
Cristiane L. Giroletti[3]
Maria Eliza Nagel-Hassemer[4]
Maria Angeles Lobo Recio[5]
Flávio Rubens Lapolli[6]

ABSTRACT

A new activated biochar was produced by carbonizing *Cássia fistula L.* leaves and its characterization was performed. Scanning Electron Microscopic (SEM) images of the activated biochar showed morphology with numerous irregular cavities and pores. BET surface area and total pore volume of produced adsorbent were 192 $m^2.g^{-1}$ and 0.108 $cm^3.g^{-1}$, respectively. Mean porous diameter of the produced biochar was 2.263 nm, characterizing a mesoporous material. Crystallinity and functional groups of the adsorbent were determined by X-ray diffraction (XRD) and Fourier Transform Infrared (FTIR) spectroscopy analyses, respectively. The pH of zero charge point (pH_{zcp}) observed was equal to 10, demonstrating that the activated biochar has a negative surface, which facilitates the adsorption of positively charged compounds in water and wastewater treatment. Tree leaves of *Cássia fistula L.* represent a promising raw material for activated biochar production, given their availability and characteristics of the adsorbent produced. The use of tree leaves for activated biochar production can reduce the operational costs of adsorption process, besides providing the use of a residue for a more noble purpose.

Keywords: Activated biochar; Tree leaves; *Cássia fistula L.*; Adsorbent characterization.

[1] Doutora em Engenharia Ambiental pela Universidade Federal de Santa Catarina (UFSC) e Pós-doutoranda pelo Departamento de Engenharia Sanitária e Ambiental – CTC – UFSC.
[2] Doutora em Engenharia Química e pós-doutoranda do Programa de Pós-Graduação em Engenharia Química na Universidade Federal de Santa Catarina (PósENQ/UFSC).
[3] Doutoranda em Engenharia Ambiental no Programa Pós-Graduação em Engenharia Ambiental na Universidade Federal de Santa Catarina (UFSC).
[4] Doutora em Química pela Universidad Complutense de Madrid, UCM, Espanha. Professora adjunta da Universidade Federal de Santa Catarina (UFSC), Campus Universitário de Araranguá.
[5] Doutora em Engenharia Ambiental pela Universidade Federal de Santa Catarina (UFSC). Professora adjunta no departamento de Engenharia Sanitária e Ambiental da Universidade Federal de Santa Catarina (UFSC).
[6] Doutor em Engenharia Hidráulica e Saneamento pela Universidade de São Paulo (USP). Professor adjunto no departamento de Engenharia Sanitária e Ambiental da Universidade Federal de Santa Catarina (UFSC).

1 INTRODUCTION

Conventional activated carbon is a known porous material with high specific surface area, fast adsorption kinetics, and high adsorptive capacity (Saka, 2012). However, due to its high cost of production and regeneration, large-scale application is limited with an increase in interest in organic matrix alternatives. These matrixes are in line with sustainable development and reduce the total cost of production of activated carbons (DURAL *et al*., 2011; *ROVANI et al*., 2016).

Agricultural and biomass residues are considered cheap and abundant raw materials with high potential for adsorption applications (NOR *et al.,* 2013, KANKILIÇ *et al.,* 2016; AHMED, 2017). In addition, the conversion of these residues into value-added products such as activated carbon could solve environmental problems such as accumulation of agricultural waste, water and air pollution, as well as being efficient in the adsorption of pollutants (Nor et al., 2013). In the last years, numerous studies have reported the use of activated carbon obtained through the use of residues of different biomasses, such as rice husk (KALDERIS *et al.,* 2008), tobacco residues (KILIC; APAYDIN-VAROL; PUTUN, 2011), orange peel (KOSEOGLU; AKMIL-BASAR, 2015), apple bagasse (ROVANI *et al.,* 2016), *Phragmites australis* (KANKILIÇ *et al.,* 2016; AHMED, 2017) and shell of fruits (ISLAM *et al*., 2017). Among the various biomass residues studied, tree leaves have also been considered as potentially promising raw material for the production of activated carbon (SUMATHI *et al.,* 2009; NOR *et al*., 2013; KANKILI *et al.,* 2016; AHMED, 2017).

Tree leaves are composed basically by three different compounds: cellulose, hemicellulose and lignin. The lignin is the main responsible by the adsorption process due to its high carbon content and molecular structure similar to bituminous coal (SUHAS *et al*., 2007; ROSS; POSSETI, 2018). Recent studies have indicated satisfactory results in the removal of pollutants by the adsorption process with leaves of *Posidonia oceanica L.* (DURAL *et al.,* 2011), palm (*Pinus brutia Ten.*) (DENIZ; KARAMAN, 2011; SOLIMAN *et al*., 2016), Ginkgo (*Ginkgo bibola*) (ZHU *et al.,* 2018), and pineapple (*Ananas comosus*) (BELTRAME *et al*., 2018). However, more researches are necessary to evaluate different conversion techniques of these biomasses into adsorbents, and its characterization.

Cássia fistula L. is a species native to India, found in several countries such as Mexico, South Africa, China and Brazil (VIEGAS JR. *et al.,* 2006). Some parts of *Cássia fistula L.* trees (stem bark, branches, pods, and internal pods mass) have been the focus of studies on production of low cost adsorbents (Senniappan et al., 2016; Sikri et al., 2018). However, adsorbents produced with leaves of *Cassia fistula L.* have not been studied in adsorption processes.

In the present study a new activated biochar was produced from leaves of *Cassia fistula L.* using the physical activation. The produced adsorbent was characterized by structural, textural and morphological analysis. The greater novelty of the present study is the production of an activated biochar from a low cost residue using only physical activation technique. This activation type is considered a sustainable technique, since chemical activation is not ecologically correct due the possibility of production of numerous undesirable, dangerous, and corrosive compounds. Furthermore, physical activation allows greater control over the development of microporosity and it eliminates the use of chemicals, reducing process costs and associated pollution.

2 MATERIALS AND METHODS

2.1 Production of the Activated Biochar

A cleaning step on leaves of *Cássia fistula L.* (collected after their natural fall) was performed with distilled water in order to remove any residue and particulate matter. The cleaned leaves passed by two drying stages: at room

temperature and in an oven for 48 hours at 60 ± 5°C. Posteriorly, the material was crushed and sieved to obtain a homogeneous mixture. The activation process was realized by carbonization, with a heating rate of 10ºC.min^{-1} until 800ºC (held for 1 hour). Afterward, the produced activated biochar was stored in an airtight container for later use.

2.2 Activated Biochar Characterization

The carbonization process of *Cássia fistula L.* leaves was evaluated by a thermogravimetric analyzer (STA 449 F3 Jupiter®) in an atmosphere of N_2 with a volumetric flow rate of 20 ml.min^{-1}, scan interval of 30 – 800°C, and a heating rate of 10°C.min^{-1}. The granulometric analysis was performed using a sieving machine with vibratory table (Bertel Metallurgic) and a standard Tyler series with sieves of 230 to 40 mesh. The mass of the fractions retained in each sieve was measured and the mean diameter was calculated as the weighted average of the fractions.

Qualitative analysis of surface functional groups was analyzed by using Fourier Transform Infrared Spectroscopy (FTIR) (IR Prestige – 21, Shimadzu) over the scan range of 4,000 to 400 cm^{-1}. The identification of the crystalline phases formed during the activated biochar synthesis was realized by X-ray diffraction (XRD) (X'Pert PRO, PANanalytical), with Cu-Kα radiation source over a diffraction angle (2θ) range between 30 and 110°, operated at 45 kV and 40 mA, with step of 0.33° every 20 seconds.

The surface morphology and existing elements of the adsorbent were observed by Scanning Electron Microscope (SEM) (JEOL JSM-6390 LV) with an auxiliary energy dispersive X-ray spectroscopy (EDS). Specific surface area (S_{BET}) and pore volume of the activated biochar were determined by physical N_2 adsorption-desorption at 77 K using an auto-adsorption system (Autosorb IC, Quantachrome) with the Brunauer–Emmett–Teller (BET) model.

The pH of zero charge point (pH_{PZC}) was determined using the batch equilibrium method by loading 50 mg of adsorbent into 50 ml of distilled water with different initial pH values (1 to 12). The pH values were adjusted by the addition of 0.1M HCl solution or 0.1M NaOH solution. The final pH was measured

after 24 h and the pH_{PZC} value was determined as the point where initial pH was equal to final pH.

3 RESULTS AND DISCUSSIONS

3.1 Thermogravimetric Analysis

The behavior of the thermal degradation of the material produced from the leaves of *Cassia fistula L.* is presented in Figure 1. The thermogravimetric curves represented by the TG and DTG curves represent the loss of the material mass as a function of the increase in temperature value. The mass loss in the range I refers to the dehydration of the material associated with evaporation of free and physically adsorbed water in the material (Sahnoun and Bouaziz, 2012). Thermal degradation started at 200ºC, indicating good thermal stability as shown by the TG curve and mass loss of approximately 60%. The interval between 300 and 400°C is attributed to the thermal degradation of cellulose and most part of the lignin. The structure of greater stability of the sample was the lignin and its degradation occurred together with the cellulose, without the formation of by-products (SEO *et al.,* 2010). The third mass loss, in the range of 600 to 700°C, corresponds to the final degradation of lignin and final structure of the adsorbent (TONGPOOTHORN *et al.,* 2011). This behavior with three mass loss intervals was also observed in adsorbents from rice husks (Suzuki et al., 2007), wood sawdust (SEO *et al.,* 2010), wheat straw (Nani et al., 2010), cashew leaves (PEREIRA, 2017) and peanut hulls (SILVA *et al.,* 2018).

Figure 1. TG (—) and DTG (---) curves of *Cássia fistula L.* leaves.

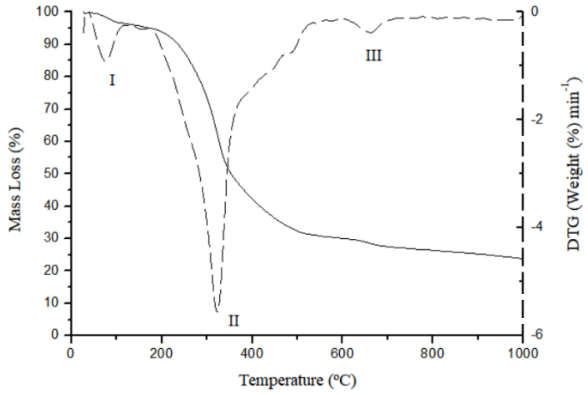

Fonte: Elaborado pelos autores, 2019.

3.2 Granulometric Analysis

The particles mass fraction retained in each sieve of the Tyler series were determined based on the granulometric analysis of the activated biochar. The particle size distribution curve of the produced adsorbent was obtained, as presented in Figure 2. Approximately 77% of the particles were retained between sieves of 100 and 60 mesh, with an average diameter of 0.15 and 0.25 mm. Particles with mean diameter lower than 0.1 mm corresponded to 23% of the sample mass. This fraction of smaller particles is desired in adsorbents since the adsorption process efficiency is favored (SEKAR *et al*., 2004).

Figure 2. Particle size distribution of the produced adsorbent: retained fraction (—) and cumulative fraction (---).

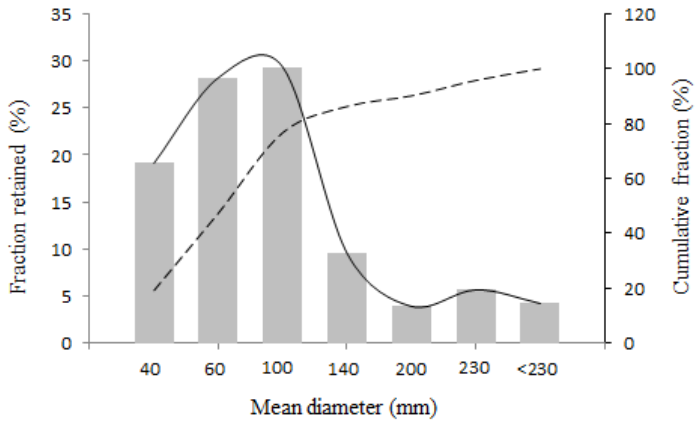

Fonte: Elaborado pelos autores, 2019.

3.2. Morphological Analysis – SEM and EDS

Scanning Electron Microscope (SEM) analysis of the activated biochar sample is essential to understand its global morphology and microscopic porous structure, as shown in Figure 3. The adsorbent produced from leaves of *Cassia fistula L.* has a porous structure, with some irregular channels and, in some parts, organized crystalline cellulose microfibrils, indicating the fibrous nature of lignocellulosic materials, even after the carbonization process (BELTRAME *et al*., 2018). Similar morphological structure were found by Zhou et al. (2017) in the *Phragmites australis* activated carbon synthesis, in which part of the channel

structures of the original material were preserved after the carbonization and activation processes.

Figure 3. SEM micrographs of the produced biochar with magnification of x1,000.

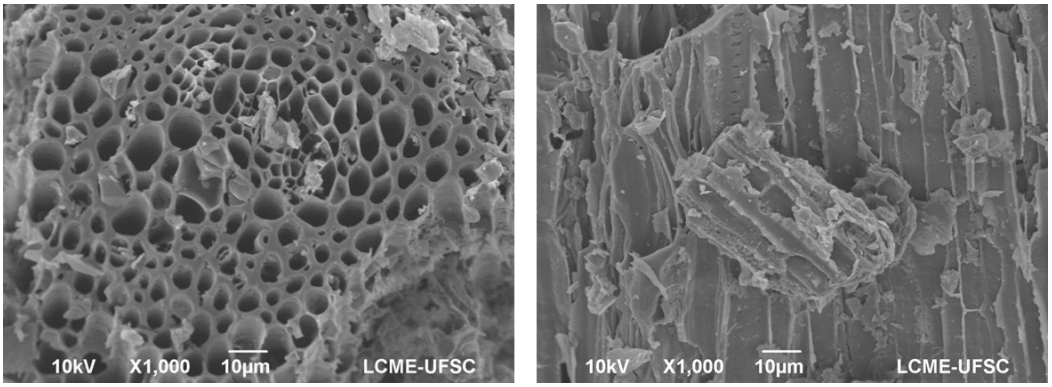

Fonte: Elaborado pelos autores, 2019.

Regarding the EDS analysis of the activated biochar, the main elements quantified in descending order were: carbon (72%), calcium (16.8%), and oxygen (10%), as presented in Figure 4. The contribution of carbon and oxygen elements in the activated biochar represents a percentage above 80%. Similar results were obtained by Ravulapalli and Kunta (2017) with an adsorbent produced of *Ficus racemosa* peel. The high percentage of these elements confirms the carbonaceous characteristic of agricultural by-product adsorbents.

Figure 4. EDS spectra of the activated biochar of *Cássia fistula L*. leaves.

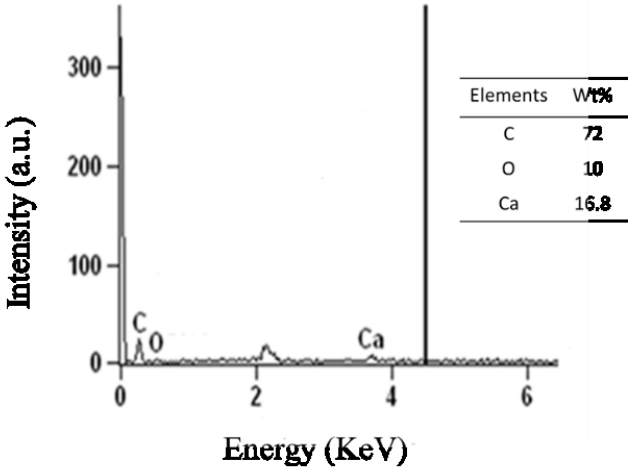

Fonte: Elaborado pelos autores, 2019.

All plants require the same basic nutrients, differentiating the efficiency of absorption and preference for certain chemical elements among each species,

which differentiates their absolute concentration and relative proportions of elements in each plant (BOTHE; SLOMKA, 2017). Calcium (Ca) is an intermediate micronutrient that, when found in excess or deficient, may be detrimental to the biochemical functions and growth of the plant, besides modifying soil pH and cation exchange capacity (REN *et al*., 2019).

3.3. Porous Structure Characterization

S_{BET} and pore volume of the produced adsorbent by *Cássia fistula L*. leaves were 192 $m^2.g^{-1}$ and 0.108 $cm^3.g^{-1}$, respectively. These results corroborate with conclusions of the SEM images, where the biochar morphology presented more aggregated particles and consequently a larger surface area. The produced activated biochar presented a mean porous diameter of 2.263 nm and was classified as a mesoporous adsorbent, in the transition range between micro and mesoporous. This study revealed that the surface area of the activated biochar produced from *Cássia fistula L.* leaves was higher than those found in adsorbents prepared with different leaves, such as, *Posidonia oceanica L.* (38.9 $m^2.g^{-1}$) (Dural et al., 2011), *Pinus brutia Ten* leaves activated with sulfuric acid (64.12 $m^2.g^{-1}$) (Soliman et al., 2016), and *Ananas comosus* leaves activated with phosphoric acid (25 $m^2.g^{-1}$) (BELTRAME *et al*., 2018).

3.4. Structural Analysis – FTIR and XRD

FTIR analysis (Figure 5) was used to evaluate and identify major functional groups contained in the structure of *Cássia fistula L. in natura* and the produced biochar. The bands at 3,415 cm^{-1} characterize vibrations in O-H groups presented in the cellulose. In the *in natura* sample it was possible to identify the presence of methylcellulose by detecting υ (C-H) and δ (C-H) strongly electronegative in the ortho position in absorption bands located in the spectrum at 2,920 cm^{-1}. After carbonization, it was observed the advance of a new peak of 875 cm^{-1}, corresponding to the angular deformation outside the plane of C-H, possibly by celluloses degradation. It was observed the band shift in the *in natura* sample of 1,618 cm^{-1} to 1,417 cm^{-1} in the adsorbent. They are correspondent to the C=O and C-O bonds present in the lignin structure, as well as the interactions with the

carboxylate group. The peaks of 707 cm^{-1} and 1,041 cm^{-1} represent angular deformation of C=C and axial deformation of C-O, respectively. The interactions between the phenolic O-H bonds present in the lignin structure, as well as the interactions with the unsaturated aliphatic structures, are the functional groups responsible for adsorption process (CALVETE *et al.,* 2010; CARDOSO *et al.,* 2011).

Similar bands between 1161-1027 cm^{-1} (C-O elongation vibration in cellulose and hemicellulose) and 1632 cm^{-1} (vibrations of lignin) were found in the study by Maaloul et al. (2017) with peanut shell adsorbent. Cardoso et al. (2011) studying the application of cupuaçu bark adsorbent found narrow bands in the range of 1254-1240 cm^{-1}, as well as intense bands at 1057, 1049 and 1050 cm^{-1} attributed to the elongation of phenolic compounds from lignin.

Figure 5. FTIR spectra of *Cássia fistula L*. Leaves *in natura* and the produced biochar.

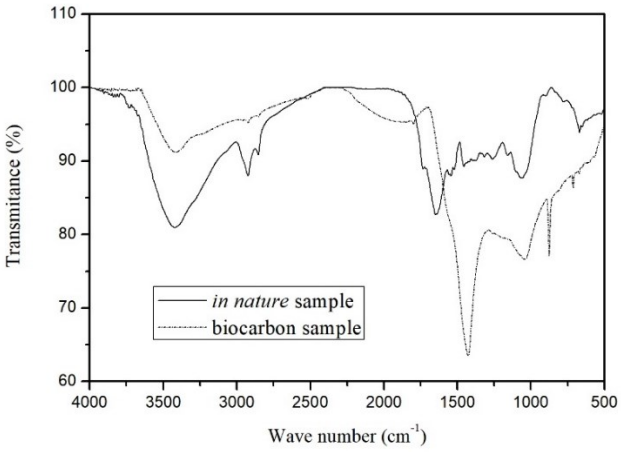

Fonte: Elaborado pelos autores, 2019.

X-ray diffraction (XRD) analysis of the adsorbent biochar informs the diffraction intensity variations, providing the fingerprint of crystalline solids presented in the activated biochar, as presented in Figure 6. High peaks in the region between 20 and 30° indicate the presence of crystalline cellulose in the samples (KEILUWEIT *et al.,* 2010). The crystallinity degree depends on the molecular arrangement of biomass and may vary mainly by the amount of lignin, cellulose, and hemicellulose from each plant (Maia et al., 2016). It is important to note that the produced adsorbent has a high degree of crystallinity and small peaks in the regions below 20º, representing highly amorphous species (PECHYEN *et al.,* 2007). The peaks around 35 and 45º correspond to reflections of disordered

micrograph structure, which are characteristics of activated carbon representing the mineral phase of carbon (SCHETINO *et al*., 2007).

Figure 6. X-ray diffraction pattern of the activated biochar of *Cássia fistula L*. leaves.

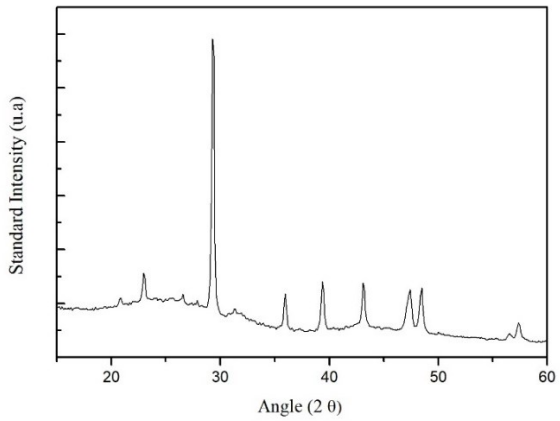

Fonte: Elaborado pelos autores, 2019.

3.5. Measurement of pH of zero charge point (pH_{ZCP})

The zero charge point of the produced activated biochar is the pH value in which the superficial charge is equal to zero, shown in Figure 7. In the experiments with initial pH between 3 and 11, it was observed a *plateau* for measured final pH (buffer effect), with the pH_{ZCP} equal to 10. The activated biochar of *Cássia fistula L.* leaves has a basic surface which is negatively charged, facilitating the adsorption of positively charged molecules. Based on these results it is possible to affirm that the contact of the adsorbent with a solution with pH less than 10 is able of promoting a negatively charged state, where a large number of cations can be absorbed. This process can be explained by the electrostatic attraction between the charge generated on the activated biochar surface and the cationic group of the solution.

Figure 7. Determinação do ponto de carga zero do biocarvão; pH inicial (—) e (pH final – pH inicial) (---).

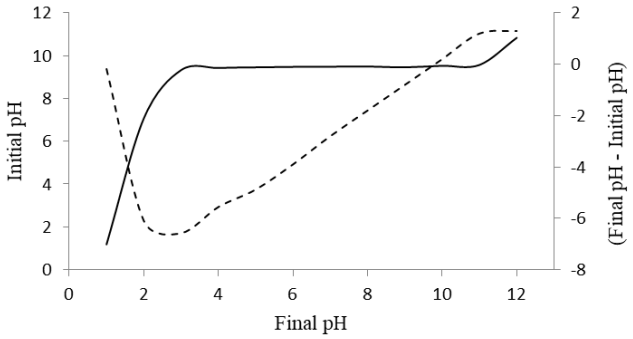

Fonte: Elaborado pelos autores, 2019.

4 CONCLUSIONS

A new activated biochar was produced by carbonizing *Cássia fistula L*. leaves. Scanning Electron Microscopic (SEM) images of the activated biochar show morphology with numerous irregular cavities and pores. BET surface area and total pore volume of produced adsorbent were 192 $m^2.g^{-1}$ and 0.108 $cm3.g^{-1}$, respectively. Mean porous diameter of the produced biochar was 2.263 nm, characterizing a mesoporous material. The high content of C (72%) and O (10%) was observed in biochar. EDS analysis imply that the raw material is a good precursor for activated biochar production. FTIR spectrum indicated the presence of carboxylate groups, which could increase the effectiveness of adsorption of several pollutants. XDR analysis provided the fingerprint of the crystalline solids presented in adsorbent, mainly crystalline cellulose. The pH of zero charge point (pH_{ZCP}) was equal to 10, demonstrating that the activated biochar has a negative surface, which facilitates the adsorption of positively charged compounds in water and wastewater treatment. Tree leaves of *Cássia fistula L.* represent a promising raw material for activated biochar production, given their availability and characteristics of the adsorbent produced. The use of tree leaves for activated biochar production can reduce the operational costs of adsorption process, besides providing the use of a residue for a more noble purpose.

ACKNOWLEDGMENTS

The authors would like to acknowledge UFSC and CAPES for the financed in part by the Coordenação de Aperfeiçoamento de Pessoal de Nível Superior – Brasil (CAPES) – Finance Code 001.

REFERENCES

AHMED, M. Application of raw and activated Phragmites australis as potential adsorbents for wastewater treatments. **Ecological Engineering**, v. 102, p. 262-269, 2017.

BELTRAME, K.K.; CAZETTA, A.L.; SOUZA, P.S.C. Adsorption of caffeine on mesoporous activated carbon fibers prepared from pineapple plant leaves. **Ecotoxicology and Environmental Safety**, v. 147, p. 64-71, 2018.

BOTHE, H.; SLOMKA, A. Divergent biology of facultative heavy metal plants. **Journal of Plant Physiology**, v. 219, p. 45-61, 2017.

CALVETE, T.; LIMA, E.C.; CARDOSO, N.F. Application of carbon adsorbents prepared from Brazilian-pine fruit shell for the removal of reactive orange 16 from aqueous solution: Kinetic, equilibrium, and thermodynamic studies. **Journal of Environmental Management,** v. 91, p. 1695-1706, 2010.

Cardoso, N.F.; Lima, E.C.; Pinto, I.S.; AMAVISCA, C.V.; ROYER, B.; PINTO, R.B.; ALENCAR, W.S.; PEREIRA, S.F.P. Application of cupuassu shell as biosorbent for the removal of textile dyes from aqueous solution. **Journal of Environmental Management,** v. 92, p. 1237-1247, 2011.

DENIZ, F.; KARAMAN, S. Removal of Basic Red 46 dye from aqueous solution by pine tree leaves. **Chemical Engineering Journal**, v. 170, p. 67-74, 2011.

DURAL, U.M.; CAVAS, L.; PAPAGEORGIOU, S.K., KATSAROS, F.K. Methylene blue adsorption on activated carbon prepared from *Posidonia oceanica* (L.) dead leaves: Kinetics and equilibrium studies. **Chemical Engineering Journal**, v. 168, p. 77-85, 2011.

ISLAM, M.A.; SABAR, S.; BENHOURIA, A.; KHANDAY, W.A.; ASIF, M.; HAMEI, B.H. Nanoporous activated carbon prepared from karanj (*Pongamia pinnata*) fruit hulls for methylene blue adsorption. **Journal of the Taiwan Institute of Chemical Engineers**, v. 74, p. 96-104, 2017.

KALDERIS, D.; BETHANIS, S.; PARASKEVA, P.; DIAMADOPOULOS, E. Production of activated carbon from bagasse and rice husk by a single-stage chemical activation method at low retention times. **Bioresource Technology**, v. 99, p. 6809-6819, 2008.

KANKILIÇ, G.B.; METIN, A.U.; TUZUN, I. Phragmites australis: An alternative biosorbent for basic dye removal. **Ecological Engineering**, v. 86, p. 85-94, 2016.

KEILUWEIT, M.; NICO, P.S.; JOHNSON, M.G.; KLEBER, M. Dynamic molecular structure of plant biomass-derived black carbon (Biochar). **Environmental Science & Technology**, v. 44, p. 1247–1253, 2010.

KILIC, M.; APAYDIN-VAROL, E.; PUTUN, E. Adsorptive removal of phenol from aqueous solutions on activated carbon prepared from tobacco residues: Equilibrium, kinetics and thermodynamics. **Journal of Hazardous Materials**, v. 189, p. 397-403, 2011.

KOSEOGLU, E.; AKMIL-BASAR, C. Preparation, structural evaluation and adsorptive properties of activated carbon from agricultural waste biomass. **Advanced Powder Technology**, v. 26, p. 811-818, 2015.

LIU, Y.; WANG, Y.; ZHANG, G.; LIU, W.; WANG, D.; DONG, Y. Preparation of activated carbon from willow leaves and evaluation in electric double-layer capacitors. **Materials Letters**, v. 176, p. 60-63, 2016.

MAALOUL, N., OULEGO, P., RENDUELES, M., GHORBAL, A.; DÍAZ, M. Novel biosorbents from almond shells: Characterization and adsorption properties modeling for Cu (II) ions from aqueous solutions. **Journal of Environmental Chemical Engineering**, v. 5, p. 2944-2954, 2017.

THILAKAVATHI.; MURUGAN, P.; ABEDI, J.; MAHINPEY, N. Pyrolysis of wheat straw in a thermogravimetric analyzer: Effect of particle size and heating rate on devolatilization and estimation of global kinetics. **Chemical Engineering Research and Design**, v. 88, p. 952-958, 2010.

NOR, N.M., LAU, CHUNG, L., LEE, TEONG, K., MOHAMED, A.R. Synthesis of activated carbon from lignocellulosic biomass and its applications in air pollution control - a review. **Journal of Environmental Chemical Engineering**, v. 1, p. 658-666, 2013.

OULD-IDRISS, A.; STITOU, M.; CUERDA-CORREA, E.M.; FERNÁNDEZ-GONZÁLEZ, C.; MACÍAS-GARCÍA, A.; ALEXANDER-FRANCO, M.F.; GÓMEZ-SERRANO, V. Preparation of activated carbons from olive-tree wood revisited. I. Chemical activation with H_3PO_4. **Fuel Processing Technology**, v. 92, p. 261-265, 2011.

PECHYEN, C.; ATONG, D.; AHT-ONG, D.; SRICHAROENCHAIKUL, V. Investigation of pyrolyzed chars from physic nut wast for the preparation of

activated carbon. **Journal of Solid Mechanics and Materials Engineering**, v. 1, p. 498-507, 2007.

RAVULAPALLI, S.; KUNTA, R. Deflouoridation studies using active carbon derive from the barks of *Ficus racemosa* plant. **Journal of Fluorine Chemistry**, v. 193, p. 58-66, 2017.

REGALBUTO, J.R.; ROBLES, J. The engineering of Pt/Carbon catalyst preparation for application on proton exchange fuel cell membrane (PEFCM). **University of Illinois: Chicago***,* 2004.

REN, H.; ZHOU, Q.; ELE, J.; HOU, Y.; JIANG, Y.; RODRIGUES, J.L.M.; CABB, A.B.; WILSON, G.W.T.; HU, J.; ZHANG, Y. Determining landscape-level drivers of variability for over fifty soil chemical elements. **Science of the Total Environment,** v. 657, p. 279-286, 2019.

ROSS, B.Z.L.; POSSETI, G.R.C. Tecnologias potenciais para o saneamento: remoção de metais de águas de abastecimento público. **Curitiba: Sanepar**, 2018.

ROVANI, S.; RODRIGUES, A.G.; MEDEIROS, L.F.; CATALUÑA, R.; LIMA, E.C.; FERNANDES, A.N. Synthesis and characterisation of activated carbon from agroindustrial waste—Preliminary study of 17β-estradiol removal from aqueous solution. **Journal of environmental chemical engineering**, v. 4, p. 2128-2137, 2016.

SAHNOUN, R.D.; BOUAZIZ, J. Sintering characteristics of kaolin in the presence of phosphoric acid binder. **Ceramics International**, v.38, p.1–7, 2012.

SAKA, C. BET, TG–DTG, FT-IR, SEM, iodine number analysis and preparation of activated carbon from acorn shell by chemical activation with $ZnCl_2$. **Journal of Analytical and Applied Pyrolysis**, v.95, p.21–24, 2012.

SCHETINO, J.M.A.; FREITASK, J.C.C.; CUNHA, A.G.; EMMERICH, F.G.; SOARES, A.B.; SILVA, P.R.N. Preparação e caracterização de carvão ativado quimicamente a partir da casca de arroz. **Química nova**, v.30, p.1663-1668, 2007.

SEKAR, M.; SAKTHI, V.; RENGARAJ, S. Kinetics and equilibrium adsorption study of lead (II) onto activated carbon prepared from coconut shell. **Colloid and Interface Science**, v.279, p.307-313, 2004.

SENNIAPPAN, S.; PALANISAMY, S.; SHANMUGAM, S.; GOBALSAMY, S. Adsorption of Pb (II) from aqueous solution by Cassia fistula seed carbon:

Kinetics, equilibrium, and desorption studies. **Environmental Progress & Sustainable Energy**, v.36, p.138-146, 2016.

SEO, D.K.; PARK, S.S.; HWANG, J.; YU, T. Study of the pyrolysis of biomass using thermo-gravimetric analysis (TGA) and concentration measurements of the evolved species. **Journal of Analytical and Applied Pyrolysis**, v.89, p.66-73, 2010.

SIKRI, N.; DHANDA, S.; DALAL, S. Kinetics of urease inhibition by different fractions of *Cassia fistula.* **South African Journal of Botany***,* 2018*.*

SILVA, L.S.; FERREIRA, F.J.L.; SILVA, M.S.; CITO, A.M.G.L.; MENEGUIN, A.B.; SÁBIO, R.M.; BARUD, H.S.; BEZERRA, R.D.S.; OSAJIMA, J.A.; SILVA FILHO, E.C. Potential of amino-functionalized cellulose as an alternative sorbent intended to remove anionic dyes from aqueous solutions. **International Journal of Biological Macromolecules**, v.116, p.1282-1295, 2018.

SOLIMAN, A.M.; ELWY, H.M.; THIEMANN, T.; MAJEDI, Y.; LABATA, F.T.; AL-RAWASHDEH, N.A.F. Removal of Pb (II) ions from aqueous solutions by sulphuric acid-treated palm tree leaves. **Journal of the Taiwan Institute of Chemical Engineers**, v.58, p.264-273, 2016.

SUHAS; CARROT, P.J.M.; CARROT, M.M.L.R. Lignin – from natural adsorbent to activated carbon: A review. **Bioresource Technology**, v.98, p.2301-2312, 2007.

SUMATHI, S.; BHATIA, S.; LEE, K.T.; MOHAMED, A.R. Optimization of microporous palm shell activated carbon production for flue gas desulphurization: Experimental and statistical studies. **Bioresource Technology**, v.100, p.1614-1621, 2009.

SUZUKI, R.M.; ANDRADE, A.D.; SOUSA, J.C.; ROLLEMBERG, M.C. Preparation and characterization of activated carbon from rice bran. **Bioresource Technology**, v.98, p.1985-1991, 2007.

TONGPOOTHORN, W.; SRIUTTHA, M.; HOMCHAN, P.; CHANTHAI, S.; RUANGVIRIYACHAI, C. Preparation of activated carbon derived from *Jatropha curcas* fruit shell by simple thermo-chemical activation and characterization of their physico-chemical properties. **Chemical Engineering Research and Design**, v.89, p.335-340, 2011.

VIEGAS JR, C.; REZENDE, A.; SILVA, D.H.S.; CASTRO-GAMBÔA, I.; BOLZANI, V.S.; BARREIRO, E.J.; MIRANDA, A.L.P.; ALEXANDRE-MOREIRA,

M.S.; YOUNG, M.C.M. Aspectos Químicos, Biológicos e Etnofarmacológicos do Gênero Cassia. **Química Nova**, v.29, p.1279-1286, 2006.

ZHOU, L.; YU, Q.; CUI, Y.; XIE, F.; LI, W.; LI, Y.; CHEN, M. Adsorption properties of activated carbon from reed with a high adsorption capacity. **Ecological Engineering**, v.102, p.443-450, 2017.

ZHU, X.; YU, S.; XU, K.; ZHANG, Y.; ZHANG, L.; LOU, G.; WU, Y.; ZHU, E.; CHEN, H.; SHEN, Z.; BAO, B.; FU, S. Sustainable activated carbons from dead ginkgo leaves for supercapacitor electrode active materials. **Chemical Engineering Science**, v.181, p.36-45, 2018.